Expanding the Substrate Scope of Acyltransferase LovD9 for the Biosynthesis of Statin Analogues

Guillermo García-Marquina,[a,b] Reyes Núñez-Franco,[c] Daniel Grajales-Hernández,[b] Gonzalo Jiménez-Osés*[c,d] and Fernando López-Gallego*[b,d]

[a] Dr. G. García-Marquina
Departamento de Química
Universidad de La Rioja
Centro de Investigación en Síntesis Química, E-26006 Logroño, Spain
E-mail: gmarquina@neb.com

[b] Dr. G. García-Marquina, Dr. D. Grajales-Hernández, Prof. F. López-Gallego
Center for cooperative Research in Biomaterials (CIC biomaGUNE)
Basque Research and Technology Alliance (BRTA)
Paseo de Miramón, 182, 20014 Donostia-San Sebastián

[c] R. Núñez-Franco, Prof. G. Jiménez-Osés
Center for Cooperative Research in Biosciences (CIC bioGUNE)
Basque Research and Technology Alliance (BRTA)
Bizkaia Technology Park, Building 800, 48160 Derio, Spain

[d] Prof. G. Jiménez-Osés, Prof. F. López-Gallego
Ikerbasque, Basque Foundation for Science
48009 Bilbao, Spain.
E-mail: gjoses@cicbiogune.es, flopez@cicbiomagune.es
URL: https://flg802.wixsite.com/flopezgallego https://www.cicbiogune.es/people/gjoses

Abstract: This study identifies new acyl donors for manufacturing statin analogues through the acylation of monacolin J acid by the laboratory evolved acyltransferase LovD9. Vinyl and *p*-nitrophenyl esters have emerged as alternate substrates for LovD9 acylation mechanism. While vinyl esters can reach product yields as high as the ones obtained by α-dimethyl butyryl-*S*-methyl-3-mercaptopropionate (DMB-SMMP), the thioester for which LovD9 was evolved, *p*-nitrophenyl esters display a reactivity even higher than DMB-SMMP for the first acylation step yet the acylation product yield is lower. The reaction mechanisms were elucidated through quantum mechanics (QM) calculations.

Introduction

Simvastatin (SVA) is a semi-synthetic analogue of the fungal polyketide lovastatin (LVA), produced by *Aspergillus terreus*. These compounds, which belong to the family of statins, entail a big pharmaceutical value as cholesterol-lowering drugs since they inhibit hydroxy methyl glutaryl coenzyme A (HMG-CoA) reductase.[1] Thus, a previous research focused on heterologous genes combination for novel statin biosynthesis.[2] Another work explored the substrate scope of wild-type acyltransferase LovD, which naturally acylates Monacolin J acid (MJA) to yield lovastatin aided by an acyl carrier protein (LovF-ACP).[3] Synthetic surrogates, such as acyl-CoA, N-acetyl cysteamine (SNAC) and methyl thioglycolate (SMTG) thioesters were successfully used as acyl donors, substituting the *S*-acyl-LovF native ACP. However, the catalytic efficiency of LovD towards these acyl donors was too low, emerging a substrate inhibition induced by the acyl acceptor (MJA) that limited the overall kinetics of the wild-type enzyme (Scheme 1). A later study identified α-dimethyl butyryl-*S*-methyl-3-mercaptopropionate (DMB-SMMP) as a superior acyl donor that showed a 30-fold higher k_{cat} value than its previous analogues, and a Michaelis constant (K_M) slightly lower than the one of MJA, avoiding substrate inhibition.[4] Then, LovD was subjected to directed evolution to improve the enzyme catalytic turnover rate towards DMB-SMMP.[5, 6] The optimized variant LovD9 displayed a 120-fold higher k_{cat} than the wild-type. As demonstrated in previous work, directed evolution not only enhanced the synthetic capability of LovD but also reduced the inhibitory effect of MJA and the competing hydrolysis of the final product.[7] This process has been intensified through the immobilization of this enzyme on solid materials for the continuous production of simvastatin.[8]

Other activated acyl donors that can be accepted by acyltransferases have been described in the literature. Enol esters, such as vinyl derivatives, are by far the most used acyl donors.[9] After acyl transfer, the leaving enol tautomerizes to its keto form thus making the reaction irreversible.[10] Vinyl esters are often liquid at reaction temperatures and used on large scale and even under solvent-free conditions.[11] In biocatalysis, they

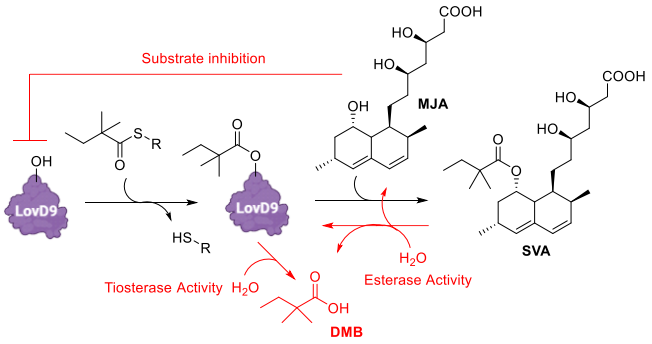

Scheme 1. Simvastatin acid (SVA) synthesis mechanism and undesired side-reactions (in red). DMB: dimethylbutyric acid; MJA: Monacolin J acid; SVA: Simvastatin acid.

have been used in the lipase-catalyzed acylation of alcohols, the synthesis of terpenyl esters through transesterification,[12] the kinetic resolution of amines, cyanohydrins and alkynols catalyzed by acyltransferases,[13] or the cell-free biosynthesis of β-hydroxy acids.[14] On the other hand, *p*-nitrophenyl (*p*NP) esters are also normally cheaper than classical enzyme acyl donors such as acyl-CoA derivatives, and they can be easily generated from commercially available carboxylic acids through a very efficient procedure using *p*-nitrophenyl chloroformate.[15, 16] *p*NP esters have been used as acyl donors for the lipase-catalyzed synthesis of anticancer drug temsirolimus[17] as well as for the synthesis of ethyl acetate catalyzed by acyltransferases.[18] In this study we have selected both vinyl and *p*NP esters with different substitution patterns as potential substrates for the acyl-transfer reaction catalyzed by LovD9.

Results and Discussion

Attempting to expand the synthetic scope of the engineered LovD9 variant in its pure form (Figure S1),[6] we assayed chemically diverse acyl donors, such as ethyl acetate (**1**), vinyl acetate (**2**), vinyl propionate (**3**), vinyl butyrate (**4**), vinyl benzoate (**5**), *p*-nitrophenyl butyrate (**6**), *p*-nitrophenyl 2-methyl butyrate (**7**), *p*-nitrophenyl 2,2-dimethyl butyrate (**8**) and DMB-SMMP (**9**) (Figure 1a). In a first screening, we assayed three acyl acceptor:donor molar ratios (1:1, 1:10 and 1:100). For all acyl donors tested at 1:100 molar ratios, the yield of the statin analogues was higher than 90%, except for **1**, **6** and **7**. **1** was unproductive under the tested acyl acceptor:donor ratios. The low reactivity of **1** was also reported for the amidation of E-cynamylamide catalyzed by the acyltransferase from *Mycobacterium smegtatis* (MsAcT).[19] On the other hand, LovD9 was inactive with **2** at 1:1 molar ratio, but achieved 15% and 95% acylation yields at 1:10 and 1:100 ratios, respectively (Figure 1b). Remarkably, LovD9 yielded the monoacetylated compounds as major products when using **2** as acyl donor, but diacetylated MJA could also be detected (Figure S2a-d). When longer and bulkier vinyl esters were used, the regioselectivity of LovD9 towards the aryl C8 hydroxyl position notably increased (Figure S2) and consequently, the monoacylated compound was the only product. Hence, we suggest that bulkier acyl groups generate steric hindrances within the LovD9 active site, limiting the subsequent acylation of other hydroxyl groups in the MJA skeleton. For linear aliphatic acyl donors (**3** and **4**), the acylation yield increased more than two-fold at acyl acceptor: donor ratios higher than 1:10 (Figure 1b). A similar trend was found when using benzoyl donors (**5**). In contrast, *p*NP derivatives such as **6** and **7** provided much lower yields (around 20%) regardless of the acyl acceptor:donor molar ratio. Nevertheless, introducing a second methyl group at the α-carbon of the *p*NP derivative aliphatic chain (**8**) increased acylation yield up to 35% and 95% at 1:10 and 1:100 molar ratios, respectively. Finally, **9** afforded similar yields as vinyl esters: 44% and 96% at 1:1 and 1:100 acyl acceptor:donor molar ratios, respectively (Figure 1b).

As we previously reported,[7] LovD9 can also perform the unwanted hydrolysis of the acyl donor limiting the product yield. To assess whether LovD9 was hydrolyzing more efficiently **6** and **7** than **8**, we incubated these acyl donors with the enzyme in absence of MJA. Figure 1c shows that more *p*-nitrophenol (*p*NP) is formed using **6** and **7** than **8**. This result aligns with the higher acylation yields achieved with this latter acyl donor. Therefore, LovD9 seems to hydrolyze linear *p*NP esters more rapidly than transfer them to the MJA, which explains why the acylation yield is significantly lower than using its branched

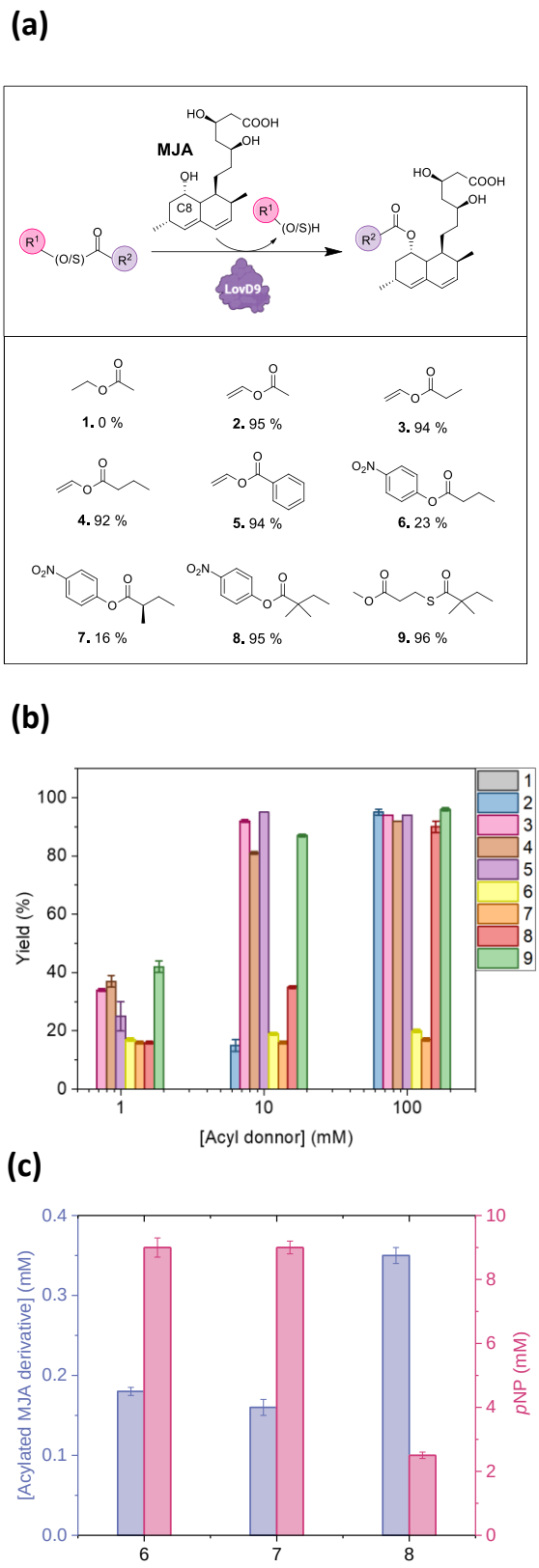

Figure 1. (a) Different substrates used in this study, highlighting the acyl group (R2), the leaving group (R1) and the acyl acceptor (MJA). C8 of MJA is the preferred position where LovD9 acylates this substrate Ethyl acetate (1), vinyl acetate (2), vinyl propionate (3), vinyl butyrate (4), vinyl benzoate (5), *p*-nitrophenyl butyrate (6), *p*-nitrophenyl (S)-2-methyl butyrate (7), *p*-nitrophenyl 2,2-dimethyl butyrate (8), α-dimethylbutyryl-S-methyl-3-mercaptopropionate (9) and monacolin J acid (MJA). Below the chemical formula of each acyl donor the yield of the statin product is provided using 100 mM acyl donor and 1 mM MJA after a 24 h reaction. **(b)** Acylation yields after 24-hour reactions with 3 μM LovD9, 1 mM MJA at increasing concentrations (1, 10 and 100 mM) of different acyl donors (1-9). **(c)** Concentration of *p*-nitrophenol (pNP) and statin derivative after 24-hour reactions with 1 μM LovD9, 1 mM MJA and 10 mM *p*-nitrophenyl ester (6, 7 or 8).

counterpart for which the unwanted hydrolysis was more limited. This hydrolase capability has been detailed previously for many acyltransferases[20] and specially for LovD9 by us.[7]

To further investigate how the different acyl donors affect the intrinsic kinetics of LovD9, we determined its Michaelis-Menten parameters (K_M and k_{cat}) towards different substrates (Figure S3 and Table S4). We selected **9** as the benchmark acyl donor, since LovD9 is the result of an *in vitro* evolution using this thioester as a surrogate substrate. Initial rates were determined spectrophotometrically by measuring the release of the corresponding alcohol or thiol over time at different concentrations of acyl donor and a fixed concentration of acyl acceptor (MJA) (Scheme S1). To do so, we exploited different colorimetric assays previously developed in our group. For vinyl esters, we monitored the production of acetaldehyde upon tautomerization of the vinyl alcohol. For *p*NP esters, the release of *p*NP was easily monitored at 405 nm by UV-Vis. Finally, for the thioester acyl donor **9**, the release of the thiol is coupled to disulphide exchange with 2,2'-dithiodipyridine, releasing pyridine-2(1*H*)-thione, which was detected at 343 nm by UV-Vis. In order to better understand the effect of the acyl donor on the acylation kinetics of LovD9, we represent the K_M as a function of the k_{cat} (Figure 2). For **5**, we could not reach the enzyme saturation point under the water solubility limits of this substrate, indicating the low affinity of LovD9 towards **5**. The most efficient acyl donor for acyltransferase catalysis must fall in the right bottom corner of this plot. As observed in Figure 2 and Table S4, LovD9 exhibits K_M values one order of magnitude higher towards vinyl esters with small acyl chains (**2** and **3**) than towards butyryl donors (**4**). When compared to vinyl esters, LovD9 shows lower K_M values towards the *p*NP derivatives and thioester **9**. These results suggest that LovD9 preferably binds four-carbon thioester donors or esters with aromatic leaving groups (i.e pNP). Regarding the k_{cat}, vinyl esters showed higher turnover numbers than **9**, but the *p*NP esters turned out to be the most catalytically productive acyl donors. For example, LovD9 shows a 3-fold higher k_{cat} towards **6** than towards **4**, despite both substrates having the same acyl group. When methyl and dimethyl substituents are introduced at the α-carbon of the acyl group (**7** and **8**), the enzyme shows a significantly lower k_{cat}, indicating that it is less competent to transfer these sterically demanding acyl chains to MJA. The **4** times higher k_{cat} of LovD9 towards **8** than towards **9** cannot compensate for its higher K_M towards the former, so the catalytic efficiency of LovD9 towards **9** is still 2-fold higher than towards **8** (inlet Figure 2, Table S4). Despite showing lower K_M values than vinyl esters and higher turnover numbers than **9**, *p*NP esters with short acyl chains (**6** and **7**) lead to low statin yields after 24-hour reactions (**Figure 1a**). These results suggest that LovD9 binds *p*-nitrophenyl esters very efficiently to form the enzyme-substrate complex, however, it is hydrolyzed more efficiently than attacked by MJA, and/or the less sterically hindered statins that are formed undergone faster hydrolysis compared to simvastatin. Hence, the undesired and competing ester hydrolysis underlying the complex mechanism of LovD9 (Scheme 1) explains why *p*-nitrophenyl esters with short acyl chains (i.e **6**) are efficiently hydrolyzed with high catalytic efficiencies (Figure 2) but poorly transferred to MJA with low statin yields (Figure 1).

The differences in the experimental catalytic rate constants (k_{cat}) of LovD9 towards the different acyl donors tested in this study were investigated through quantum mechanical (QM) calculations (Figure S4, Table S5) using pivaloyl as a model for

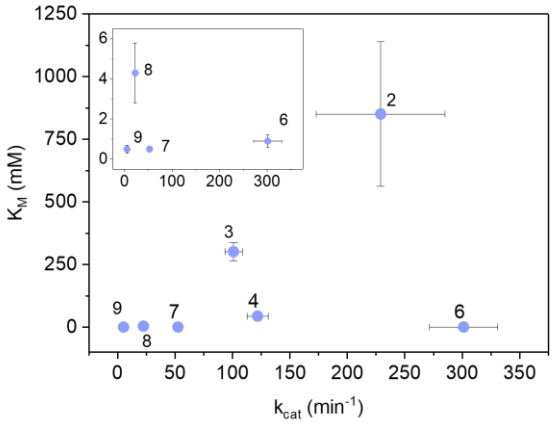

Figure 2. Kinetic parameters (K_M and k_{cat}) for the monacolin J (MJA) acylation catalysed by LovD9 using different acyl donors: vinyl acetate (**2**), vinyl propionate (**3**), vinyl butyrate (**4**), *p*-nitrophenyl butyrate (**6**), *p*-nitrophenyl (*S*)-2-methyl butyrate (**7**), *p*-nitrophenyl 2,2-dimethyl butyrate (**8**), α-dimethylbutyryl-*S*-methyl-3-mercaptopropionate (**9**), in the presence of 1 mM MJA. A zoomed-in region (0-6 mM) is displayed in the left-top corner to have a better comparison of **6**, **7**, **8** and **9** substrates.

the acyl group. Figure 3 shows that the thioester model *S*-methyl 2,2-dimethylpropanethioate, the non-activated ester model methyl pivalate and the activated ester model vinyl pivalate, undergo the canonical stepwise mechanism involving nucleophilic addition of the serine model hydroxyl to the carbonyl group followed by subsequent elimination of the leaving group (a thiol, an alcohol and an enol, respectively). As shown in Figure 3a (and Scheme S2), in all three cases, the Michaelis complex (C) entails a hydrogen bond network involving the S/O atoms of the (thiol) ester group of the acyl donor and the backbone amide of Ser76 (modelled as Ac-Ser-NHMe). The first step in the enzyme acylation reaction involves the nucleophilic attack of Ser76 hydroxyl group with neutral Lys79 (modelled as methylamine) acting as a base, to the carbonyl carbon of the acyl donor (transition states TS_{add}), leading to a negatively charged high energy tetrahedral intermediate (I). Figure 3b shows the reaction energy profiles of the different acyl donors where global activation energies are shown. Besides, we also calculated the intrinsic activation barriers from C to TS_{add} for the thioester, non-activated alkyl ester and activated vinyl ester models, giving a value of 19.4, 20.9 and 18.0 kcal mol^{-1}, respectively. These intrinsic energy barriers inform more accurately about the electronic properties and reactivity of each functional group, decoupling the activation energies from their ability to form the Michalis complex. Next, the very reactive tetrahedral intermediates quickly undergo C–S/O bond breaking and concomitant hydrogen transfer through the Lys79-Tyr188 (the later residue modelled as phenol) proton shuttle (transition states TS_{elim}). For the three models, the energy of TSelim is slightly lower than that of TS_{add}, which becomes the rate-limiting step, as occurs in the acylation of MsAcT catalytic serine.[21] The overall calculated reaction energies ($\Delta G(T\text{-}T_{Ac})$) suggest that the whole acylation reaction is slightly exergonic with thioesters and nearly thermoneutral with vinyl esters; however, acylation with non-activated esters is calculated to be highly endergonic (i.e., thermodynamically unfeasible), reflecting the properties of the leaving group in each acyl donor surrogate (for instance, the pK_a of thiols and vinyl alcohols is significantly lower than those of alkyl alcohols).

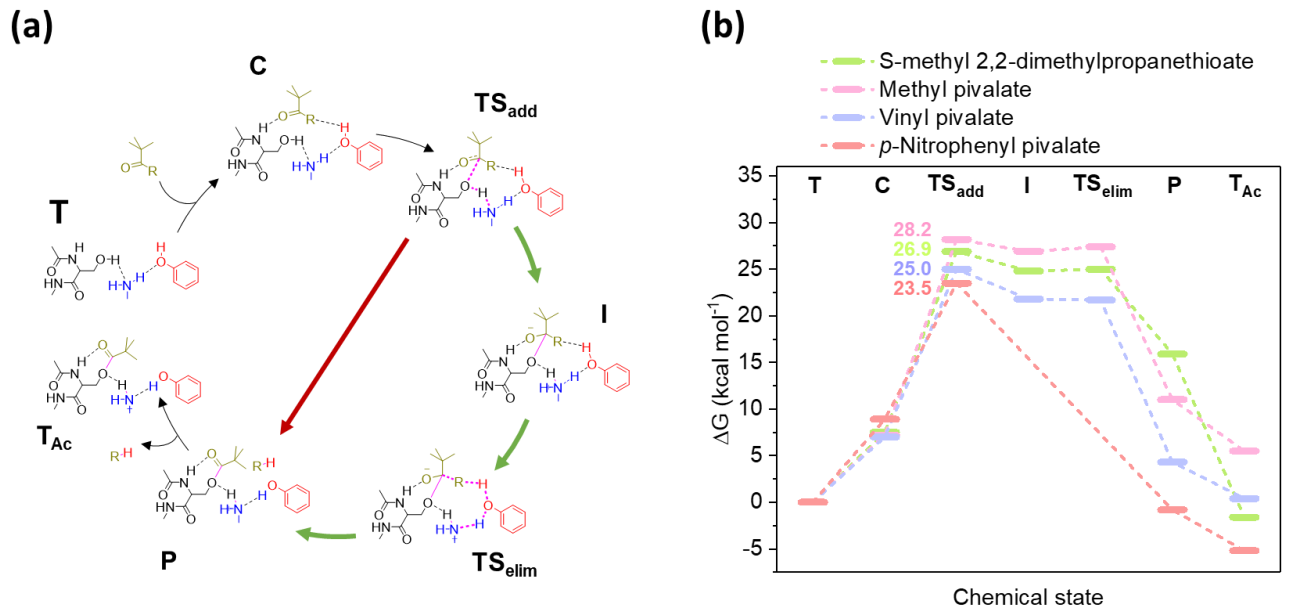

Figure 3. (a) Mechanism of LovD9 acylation. The green arrows indicate the mechanism calculated for the stepwise acylation when thioesters, vinyl esters or non-activated esters are used as donors. The red arrow indicates the concerted addition-elimination mechanism calculated when pNP esters are used as donors. **(b)** Calculated lowest-energy profiles of LovD9 catalytic triad (Ser76-Lys79-Tyr188) acylation mechanism with S-methyl 2,2-dimethylpropanethioate, methyl pivalate, vinyl pivalate and *p*-nitrophenyl pivalate using abbreviated models. The step of the reaction are defined as T: free active site, C: Michaelis complex, TS_{add}: Transition state addition, I: tetrahedral intermediate, TS_{elim}: Transition state elimination, P; product release, T_{Ac}; acetylated active site. (see ESI for further details). The global activation barriers measured from T to TS_{add} are given with the corresponding color for each acyl donor.

However, the acylation mechanism changes when a *p*NP ester model was used as an acyl donor, undergoing a concerted acyl transfer mechanism.[22-24] In this case, the *p*NP activated ester binds to the active site through the same hydrogen bond network described above, leading to a much more favored transition state (TS) with an intrinsic activation barrier of 14.6 kcal mol^{-1} involving simultaneous O–C and C–O bond formation/breaking and proton shuttling to yield the acylated Ser76 and release the *p*NP in a single step. The larger exergonic character of this reaction is related to the change in the reaction mechanism and the much lower activation energy of the process, as *p*-nitrophenoxyde is a very polarizable anion and a weak base (pK_a *p*-nitrophenol = 7.15), and hence a very good leaving group. Intrinsic Reaction Coordinate (IRC) calculations (Figure S5) support the stepwise and concerted nature of the calculated mechanisms depending on the nature of the leaving groups in the herein tested acyl donors. The calculated activation barriers are in good agreement with the experimental data, as k_{cat} values follow the same trend as the computational kinetics: *p*NP esters > vinyl esters > thioesters >> alkyl esters.

Conclusion

The development of new catalytic pathways for the biosynthesis of pharmaceutically relevant statins has been analyzed. In this work, we have characterized the broad substrate specificity of the highly active simvastatin synthase LovD9 towards different acyl donors. The k_{cat} of LovD9 towards vinyl and *p*NP esters is even higher than that of the substrate for which the enzyme was evolved (DMB-SMMP), demonstrating the enzyme's promiscuity. Vinyl esters showed much worse specific binding (K_M) than DMB-SMMP, but their high reactivity makes them suitable acyl donor candidates when used in large excess compared to the acyl acceptor. *p*NP esters displayed both good k_{cat} and K_M values, but the unwanted hydrolysis of the acyl enzyme complex outcompeted MJA acylation. However, *p*NP 2,2-dimethyl butyrate achieved simvastatin yields comparable to those of DMB-SMMP thus posing an alternative for simvastatin manufacturing. The mechanism for Ser76 acylation with different thioester/ester surrogate models was studied through QM calculations. A shift from the canonical stepwise acylation mechanism with thioesters and alkyl/vinyl esters to a concerted mechanism in the case of *p*NP esters was found. These calculations also supported the superior kinetic and thermodynamic properties of *p*NP esters when compared to the rest of the studied acyl donors, including thioesters. Therefore, our work provides valuable insights into substrate promiscuity of engineered LovD9 and into the discovery of novel substrates for statins biosynthesis.

Experimental Section

Materials and Molecular Biology Methods. LovD9 gene was synthetized and cloned into expression vector pET28b by GeneScript Gene Synthesis service (Piscataway, NJ, USA). The sequence is provided in Table S1. The genotype of the bacteria strains used for molecular biology and expression purposes are described in Table S2. Substrates monacolin J acid (MJA) and α-dimethylbutyryl-*S*-methyl-3-mercaptopropionate (DMB-SMMP) were synthetized and donated by the Tang lab (UCLA, USA). Simvastatin hydroxyl acid ammonium salt 98% was purchased from Toronto Research Chemicals (Toronto, Canada). 2,2'-Dithiodipyridine 100%, vinyl acetate, vinyl propionate, vinyl butyrate, vinyl benzoate, ethyl 2-methyl butyrate, *p*-nitrophenyl butyrate, N-(3-

dimethylaminopropyl)-N'-ethylcarbodiimide hydrochloride (EDC), yeast alcohol dehydrogenase (yADH) lyophilized powder and Amicon Ultra-0.5 centrifugal filter units (10 kDa) were purchased from Sigma-Aldrich (Merck) (St. Louis, IL, USA). Substrates *p*-nitrophenyl 2-methyl butyrate and *p*-nitrophenyl 2,2-dimethyl butyrate were synthetized in our labs. Agarose microbeads with cobalt chelates (AG-Co^{2+}) (50-150 µm diameter) were purchased from Agarose Bead Technologies (Madrid, Spain). Polypropylene (12 x 32 mm, 300 µL volume) vials were purchased from Waters (Milford, Massachusetts, USA). MicroWell 96-well microplates were purchased from Thermo Fisher Scientific (Waltham, Massachusetts, USA).

Expression and purification of LovD9. The plasmids encoding His-tagged LovD9 was transformed into chemically competent *E. coli* strains DH5α and BL21 through heat shock[25] for plasmid propagation and recombinant protein expression, respectively. Single colonies of *E. coli* containing the plasmid encoding LovD9 were inoculated into 3 mL of Lysogeny broth (LB) medium containing 30 µg mL^{-1} of kanamycin. Cells were grown overnight at 37 °C with shaking at 250 rpm. The culture was diluted 1:50 into 50 mL of LB medium containing 30 µg mL^{-1} of kanamycin and the culture was grown until OD600nm reached 0.6-0.8. At that point, the protein expression was induced by adding isopropyl-D-thiogalactoside (IPTG) to a final concentration of 0.1 mM and the culture was incubated overnight at 21 °C with shaking at 250 rpm. Cells were collected by centrifugation (2057 xg for 30 min at 4 °C) and cell pellet was resuspended with 5 mL of 50 mM sodium phosphate buffer (pH 8.0). Cells were lysed by sonication at 4 °C and cell debris was removed by centrifugation (12857 xg for 30 min).

LovD9 His-tagged protein was purified through immobilized metal affinity chromatography (IMAC) using agarose-based resin functionalized with cobalt chelates (AG-Co^{2+}) in bulk. First, the 1 mL of cell lysate was incubated with 100 mg of resin in purification buffer (50 mM 4-(2-hydroxyethyl)-1-piperazineethanesulfonic acid (HEPES), 10 mM $MgCl_2$ at pH 8) for 1 h at 4 °C, then the bound enzymes were washed with the same purification buffer and eluted with 200 mM imidazole in 50 mM HEPES 10 mM $MgCl_2$ at pH 8.0. Protein concentrations were qualitatively assessed by sodium dodecyl sulphate-polyacrylamide gel electrophoresis (SDS-PAGE) (Figure S1) and quantitatively determined by Bradford protein assay[26] using bovine serum albumin as a standard.

Synthesis of acyl donors. A 10 mL solution of N-(3-dimethylaminopropyl)-N'-ethylcarbodiimide hydrochloride (EDC; 843 mg, 440 mM) was prepared in dichloromethane (DCM). Acyl donor (408 mg for (*S*)-2-methyl butyrate and 464 mg for 2,2-dimethyl butyrate) and HCl were slowly added at room temperature to the solution until a final concentration of 400 mM for the acyl donor was reached. The mixture was stirred for 10 minutes at room temperature and 250 rpm to obtain the corresponding O-acylisourea. A 10 mL solution of *p*-nitrophenol (*p*NP; 556 mg, 400 mM) was prepared in DCM. The *p*-nitrophenol solution was then added to the O-acylisourea solution at room temperature. 4-dimethylaminopyridine (DMAP) was added as a catalyst (24 mg) to a final concentration of 10 mM. The mixture was stirred overnight at 25 °C and 250 rpm. Reaction progress was monitored through thin-layer chromatography (TLC) under UV light (254 nm). Finally, 2 volumes of hexane were added to the reaction mixture, and hydrophilic reaction by-products and unreacted *p*NP were removed by liquid -liquid extraction employing distilled water (3 x 20 mL) This process was repeated until the aqueous phase was completely transparent and the yellow colour from *p*NP had disappeared. By-products removal was monitored through TLC. Finally, the organic phase was evaporated at reduced pressure using a rotary evaporator. *p*-nitrophenyl (*S*)-2-methylbutyrate and *p*-nitrophenyl 2,2-dimethylbutyrate were obtained (49% and 45% yield, respectively).

Characterization of acyl transfer reaction with different acyl donors and acceptors through UPLC/MS. Batch reactions were carried out with 1 µM LovD9 in 50 mM HEPES, 10 mM $MgCl_2$ (pH 8) and 10 % DMSO, with different concentrations of the acyl donor (1, 10 and 100 mM) and MJA fixed at 1 mM. Acyl donors tested in this study were ethyl 2-methyl butyrate, vinyl acetate, vinyl propionate, vinyl butyrate, vinyl benzoate, *p*-nitrophenyl butyrate, *p*-nitrophenyl (*S*)-2-methyl butyrate, *p*-nitrophenyl 2,2-dimethylbutyrate and α-dimethylbutyryl-S-methyl-3-mercaptopropionate (DMB-SMMP). Reaction samples were collected after 24 hours by passing them through a tangential ultrafiltration unit (Amicon Ultra centrifugal filters, 10 kDa). Samples were analyzed by Ultra Performance Liquid Chromatography (UPLC) (Waters 2690) equipped with a Photodiod array (PDA) detector using a ACQUITY UPLC® BEH C18 1.7 µm (2.1 x 50 mm) Waters column coupled to a LCT XE time-of-flight (TOF) mass spectrometry detector with electrospray ionization source (ESI). Analytes were eluted with an isocratic mobile phase composed of 52 % (v/v) of acetonitrile in water (0.1 % (v/v) formic acid) during 15 min at flow rate of 0.3 mL min^{-1}. The source parameters of the mass spectrometer were: capillary voltage 1000 V, cone voltage 50 V, cone gas 50 L h^{-1}, desolvation gas 600 L h-1, mass range 100-1000 m/z. Source temperature was set at 120 °C. Retention times and masses of the different statins are described in Table S3.

Kinetic characterization of combined LovD9 thioesterase and acyltransferase activities with different acyl donors. Three different enzymatic assays were used to measure the kinetic parameters of LovD9-catalyzed ester conversion (combined esterase and transferase activities). For vinyl esters surrogates, acetaldehyde is generated as a by-product. The kinetics of the reaction were indirectly derived by measuring acetaldehyde conversion to ethanol by mixing 0.5 µM LovD9 with 1 µM yeast alcohol dehydrogenase (yADH) and 0.25 mM NADH.[27] NADH disappearance was monitored by UV-VIS spectroscopy at λ = 340 nm (Scheme S1a). Reactions were carried out with 1 mM MJA and different concentrations of vinyl acetate (50-500 mM), vinyl propionate (5-400 mM) or vinyl butyrate (10-400 mM). For *p*NP esters surrogates, the reaction was directly monitored by detecting *p*NP release by UV-VIS spectroscopy at λ = at 405 nm (Scheme S1b). Reactions were carried out with 1 µM LovD9, 1 mM MJA and different concentrations of *p*-nitrophenyl butyrate, *p*-nitrophenyl (*S*)-2-methyl butyrate (0.125-5 mM) or *p*-nitrophenyl 2,2-dimethyl butyrate (1-7 mM). For DMB-SMMP, reactions were monitored by detecting (*S*)-methyl mercaptopropionate (SMMP) through reaction with 4 mM 2-dithiodipyridine (2-DTDP) and subsequent pyridine-2(1H)-thione release by UV-VIS spectroscopy at λ = 323 nm (Scheme S1c).[28] Reactions were carried out with 1 µM LovD9, 1 mM MJA and different concentrations of DMB-SMMP (0.0625-3 mM). All the measurements were performed after 30 min reactions at 30 °C in 96-well plates in a BioTek Epoch2 spectrophotometer and kinetic data were fitted to the Michaelis-Menten model.

LovD9 kinetic parameters for new acyl donors. The Michaelis constant (K_M) and the turnover number (k_{cat}) for the LovD9-catalyzed ester conversion (combined esterase and transferase activities) with different acyl donors were determined spectrophotometrically from 0.5 to 400 mM depending on the acyl donor and calculated employing Origin software. All experiments were conducted in the presence of MJA at a fixed concentration to mitigate hydrolysis of the acyl-enzyme complex through the direct competition between the acyl acceptor and water.

Quantum mechanical calculations. The catalytically relevant atoms of the catalytic triad were extracted from the crystallographic structure of LovD9 (PDB 4LCM) and the rest of the functional groups were added and/or edited manually with GaussView prior to optimization. Full geometry optimizations and transition structure (TS) searches were carried out with Gaussian 165 using the M06-2X hybrid functional[29] and 6-31+G(d,p) basis set with ultrafine integration grids. Bulk solvent effects in water were considered implicitly through the IEF-PCM polarizable continuum model.[30] The possibility of different conformations was considered for all structures. All stationary points were characterized by a frequency analysis performed at the same level used in the geometry optimizations from which thermal corrections were obtained at 298.15 K. The quasi-harmonic approximation reported by Truhlar et al. was used to replace the harmonic oscillator approximation for the calculation of the

vibrational contribution to enthalpy and entropy.[31] Scaled frequencies were not considered. Mass-weighted intrinsic reaction coordinate (IRC) calculations were carried out by using the Hessian-based predictor-corrector integrator scheme by Hratchian and Schlegel[32, 33] to ensure that the TSs indeed connected the appropriate reactants and products. Gibbs free energies (ΔG) were used for the discussion on the relative stabilities of the considered structures. Free energies calculated using the gas phase standard state concentration (1 atm = 1/24.5 M) were converted to reproduce the standard state concentration in solution (1 M) by subtracting or adding 1.89 kcal mol^{-1} for bimolecular additions and decompositions, respectively. The lowest energy conformer for each calculated stationary point was considered in the discussion; all the computed structures can be obtained from authors upon request. Cartesian coordinates, electronic energies, entropies, enthalpies, Gibbs free energies, and lowest frequencies of the calculated structures are summarized in Table S5.

Conflict of Interest

The authors declare no conflict of interest.

Acknowledgements

This research was funded by Agencia Estatal de Investigación of Spain (projects CTQ2015-70524-R and RTI2018‐099592‐B‐C22 to G.J.O. and predoctoral fellowship to G.G.M). G.J.O. and F.L.G. acknowledge support from Ikerbasque. This work was performed under the Maria de Maeztu Units and Severo Ochoa Centers of Excellence Program from the Spanish State Research Agency (grants MDM-2017-0720 to CIC biomaGUNE and SEV-2016-0644 to CIC bioGUNE). We thank Prof. Yi Tang for kindly providing us with MJA, and DMB-SMMP.

Keywords: acyltransferase • biocatalysis • LovD9 • statins • substrate scope

1. E. S. Istvan, J. Deisenhofer, *Science*. **2001**, *292*, 1160-1164.
2. H. Itoh, M. Matsui, Y. Miyamura, I. Takeda, J. Ishii, T. Kumagai, M. Machida, T. Shibata, M. Arita, *ACS Synth. Biol.* **2018**, *7*, 2783-2789.
3. X. Xie, K. Watanabe, W. A. Wojcicki, C. C. C. Wang, Y. Tang, *Chem. Biol.* **2006**, *13*, 1161-1169.
4. X. Xie, Y. Tang, *Appl. Environ. Microbiol.* **2007**, *73*, 2054-2060.
5. X. Gao, X. Xie, I. Pashkov, M. R. Sawaya, J. Laidman, W. Zhang, R. Cacho, T. O. Yeates, Y. Tang, *Chem. Biol.* **2009**, *16*, 1064-1074.
6. G. Jiménez-Osés, S. Osuna, X. Gao, M. R. Sawaya, L. Gilson, S. J. Collier, G. W. Huisman, T. O. Yeates, Y. Tang, K. N. Houk, *Nat. Chem. Biol.* **2014**, *10*, 431-436.
7. G. García-Marquina, R. Núñez-Franco, F. Peccati, Y. Tang, G. Jiménez-Osés, F. López-Gallego, *ChemCatChem*. **2022**, *14*, e202101349.
8. G. García-Marquina, J. Langer, M. Sánchez-Costa, G. Jiménez-Osés, F. López-Gallego, *ACS Sustainable Chem. Eng.* **2022**, *10*, 9899-9910.
9. V. Soares, M. B. Marini, L. A. de Paula, P. S. Gabry, A. C. F. Amaral, C. A. Malafaia, I. C. R. Leal, *Biotechnol. Lett.* **2021**, *43*, 469-477.
10. M. Paravidino, U. Hanefeld, *Green Chem.* **2011**, *13*, 2651-2657.
11. L. P. Hinner, J. L. Wissner, A. Beurer, B. A. Nebel, B. Hauer, *Green Chem.* **2016**, *18*, 6099-6107.
12. R. Chênevert, N. Pelchat, P. Morin, *Tetrahedron: Asymm.* **2009**, *20*, 1191-1196.
13. N. de Leeuw, G. Torrelo, C. Bisterfeld, V. Resch, L. Mestrom, E. Straulino, L. van der Weel, U. Hanefeld, *Adv. Synth. Catal.* **2018**, *360*, 242-249.
14. A. H. Orrego, M. G. Rubanu, I. L. López, D. Andrés-Sanz, G. García-Marquina, G. E. Pieslinger, L. Salassa, F. López-Gallego, *Angew. Chem. Int. Ed.* **2023**, *62*, e202218312.
15. S. Sonkaria, G. Boucher, J. Florez-Álvarez, B. Said, S. Hussain, E. L. Ostler, S. Gul, E. W. Thomas, M. Resmini, G. Gallacher, K. Brocklehurst, *Biochem. J.* **2004**, *381*, 125-130.
16. J.-J. Li, T. D. H. Bugg, *Org. Biomol. Chem.* **2007**, *5*, 507-513.
17. X. Ju, J. Li, M. Hou, J. Tao, *Eng. Life Sci.* **2015**, *15*, 229-233.
18. C. Patinios, L. Lanza, I. Corino, M. C. R. Franssen, J. Van der Oost, R. A. Weusthuis, S. W. M. Kengen, *Front. Microbiol.* **2020**, *11*.
19. M. L. Contente, A. Pinto, F. Molinari, F. Paradisi, *Adv. Synth. Catal.* **2018**, *360*, 4814-4819.
20. H. Müller, H. Terholsen, S. P. Godehard, C. P. S. Badenhorst, U. T. Bornscheuer, *ACS Catal.* **2021**, *11*, 14906-14915.
21. M. Kazemi, X. Sheng, W. Kroutil, F. Himo, *ACS Catal.* **2018**, *8*, 10698-10706.
22. F. Ruff, Ö. Farkas, *J. Phys. Org. Chem.* **2011**, 24, 480-491.
23. A. A. Koch, D. A. Hansen, V. V. Shende, L. R. Furan, K. N. Houk, G. Jiménez-Osés, D. H. Sherman, *J. Am. Chem. Soc.* **2017**, *139*, 13456-13465.
24. A. Caneschi, D. Gatteschi, R. Sessoli, P. Rey, *Acc. Chem. Res.* **1989**, *22*, 392-398.
25. I. M. Van Die, H. E. N. Bergmans, W. P. M. Hoekstra, *Microbiol.* **1983**, *129*, 663-670.
26. M. M. Bradford, *Anal. Biochem.* **1976**, 72, 248-254.
27. S. B. Raj, S. Ramaswamy, B. V. Plapp, *Biochem.* **2014**, *53*, 5791-5803.
28. D. R. Grassetti, J. F. Murray, *Arch. Biochem. Biophys.* **1967**, *119*, 41-49.
29. Y. Zhao, D. G. Truhlar, *Theor. Chem. Acc.* **2008**, *120*, 215-241.
30. G. Scalmani, M. J. Frisch, *J. Chem. Phys.* **2010**, *132*, 114110.
31. R. F. Ribeiro, A. V. Marenich, C. J. Cramer, D. G. Truhlar, *J. Phys. Chem. B*. **2011**, *115*, 14556-14562.
32. H. P. Hratchian, H. B. Schlegel, *J. Chem. Phys.* **2004**, *120*, 9918-9924.
33. H. P. Hratchian, H. B. Schlegel, *J. Chem. Theory Comput.* **2005**, *1*, 61-69.

Entry for the Table of Contents

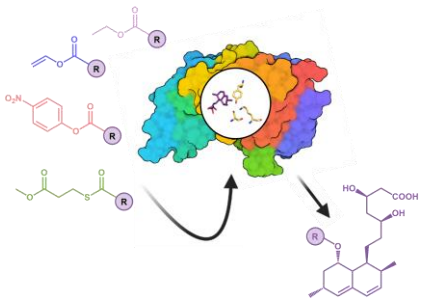

This study unveils the substrate promiscuity of acyltransferase LovD9, which turns to be very efficient by accepting vinyl and *p*-nitrophenyl derivatives as acyl donors for the obtaining of statin analogues.